ifv Bahntechnik

Interdisziplinärer Forschungs-verbund BAHNTECHNIK e.V.

European Network of Railway Competence

3rd International Symposium

RAIL-AERODYNAMICS 2018

Aerodynamics of Trains and Infrastructure

Berlin, 31 January - 1 February 2018

www.railway-network.eu/aerodynamics

INTRODUCTION of the next SPEAKER:

Thomas Thieme

Position: Research Associate

German Aerospace Center, Ground Vehicles (AS-BOA)

Göttingen/Germany

www.dlr.de/as/

3rd International Symposium on RAIL AERODYNAMICS 2018

Force and Flow Field Measurements on two Trains in Platoon Configuration

Thomas Thieme[1]

Research Associate

German Aerospace Center (DLR)

Henning Wilhelmi[1], Arne Henning[1], Claus Wagner[1,2]

[1]German Aerospace Center, Bunsenstraße 10, 37073 Göttingen

[2]Technische Universität Ilmenau, Thermo- und Fluiddynamics, Helmholtzring 1, 98693 Ilmenau

CONTENTS / OVERVIEW

FORCE AND FLOW FIELD MEASUREMENTS ON TWO TRAINS IN PLATOON CONFIGURATION

INTRODUCTION

Motivation of Platooning by Trains

- Reduction of aerodynamic drag of the platoon by driving in the wake of the leading train
  - ⟶ energy savings and hence resources and cost savings. Concept is known from sports or wildlife

Figure 1: Cyclist using wake to save energy, (www.totalwomenscycling.de, 2018)

Figure 2: NASCAR driving in wake, (www.nascar.com,2018)

- Substituting the mechanical by a virtual connection allows
  - entering and leaving the platoon in a flexible manner. Trains with the same destination can meet on track and would not have to wait at stations ⟶ decrease of waiting periods and consequently traveling time.
  - Increase of the occupation of the railway network ⟶ more passengers at the same time

What is Virtual Coupling?

- Operating trains in a platoon or convoy with no physical connection between the trains
- Automatic acceleration and breaking process of the following trains
- Communication between the trains is necessary
- Trains can enter and leave the convoy during operation without stopping at a station

  ⟶ entering and leaving the platoon can be performed highly dynamically
- Virtual Coupling is part of the Next Generation Train-Project (NGT)

Figure 3: ICE3 with mechanical connection at a station, (www.bahnbilder.de,2018)

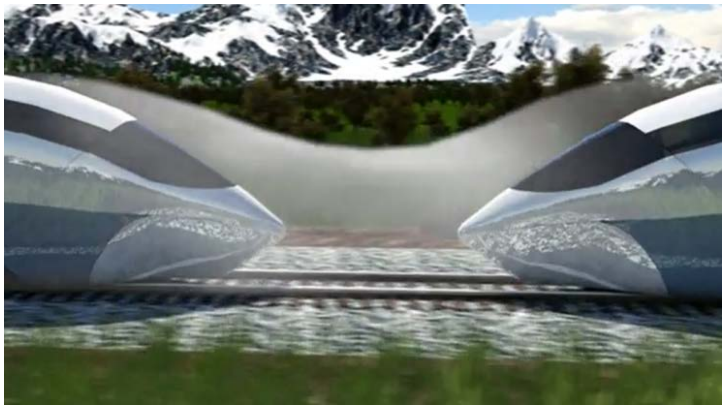

Figure 4: NGT with virtual connection, (Ben Schaub, 2016)

State of the Art

- Research work on car aerodynamic in platoons (Zabat et. al.,1995)
  - Drag reduction up to 45 %
  - Drag reduction on both cars

Further work has been carried out on

- Race cars during passing maneuvers (Romberg et. al., 1971)
- Mixed Convoys of Cars and Trucks (P. Jootel, 2014)
- Basic research work an generic bodies (Koenig und Roshko, 1985)

- The authors are not aware of publications about train aerodynamics in platoons but their own (Thieme, 2016).

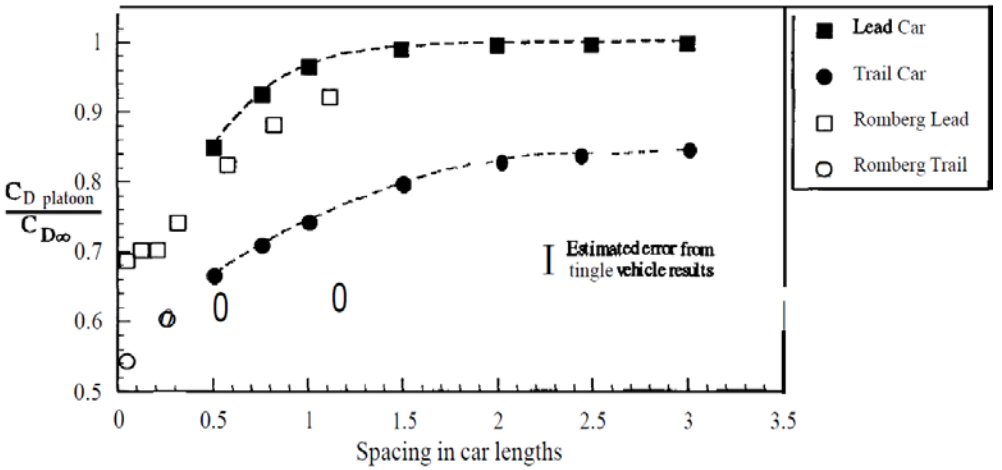

Figure 5: Aerodynamic drag of a two-car platoon, (Zabat et. al., 1995)

Figure 6: Mixed Convoy, (P. Jootel, 2014)

Questions to be Answered by this Work

1. Can the aerodynamic drag be reduced by Virtual Coupling?
2. What unsteady aerodynamic forces do occur?
3. What effect do the unsteady aerodynamic forces have on the aerodynamic drag?
4. What effect has the flow between the two trains on the aerodynamic forces?
5. How does the distance between the trains affect the aerodynamic forces?

An Approach to address this task:

An experimental investigation of the aerodynamic properties of two lined up NGT models at different distances between the trains with focus on:

1. Measurement of the aerodynamic forces with two 6-component piezo balances
2. PIV measurements of the flow field between the two train models with a vertical light sheet

All experiments were performed at the water towing tank at DLR in Göttingen.

Experimental Set-Up

Water Towing Tank Göttingen (WSG)

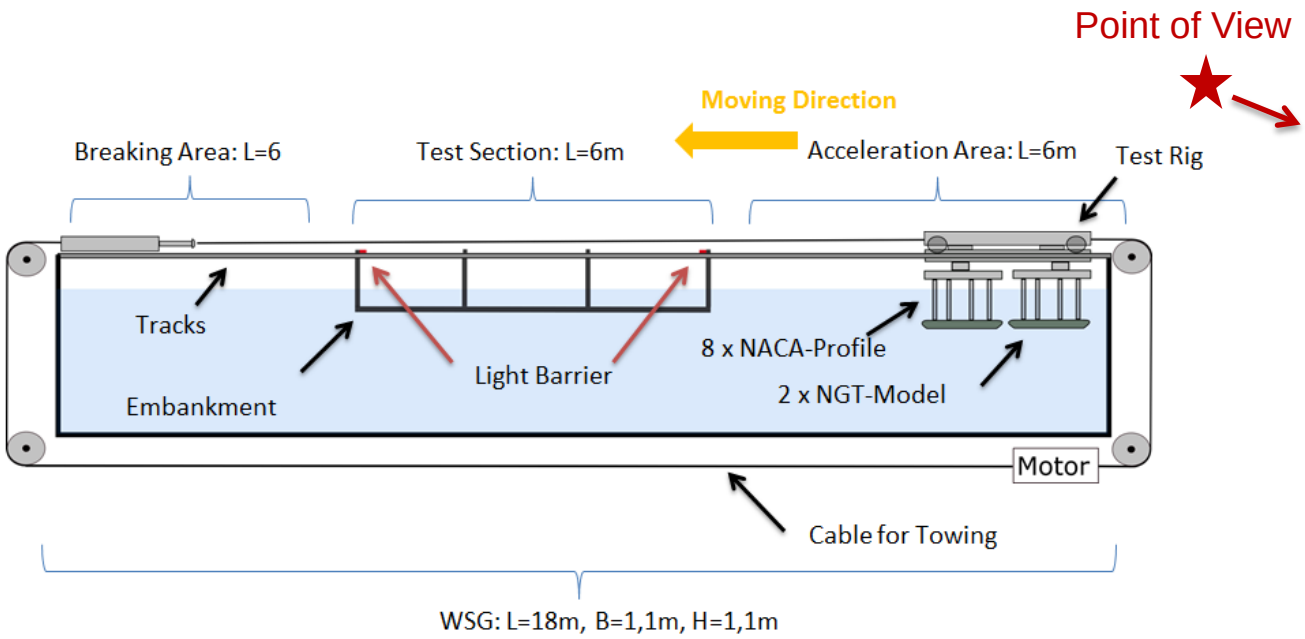

Figure 7: Schematic illustrations of the WSG with test rig and NGT2-models

WSG was used because

- of higher density of water compared to air
  → forces appear stronger
- the train model moves through fluid
  → velocity reference system is similar to reality

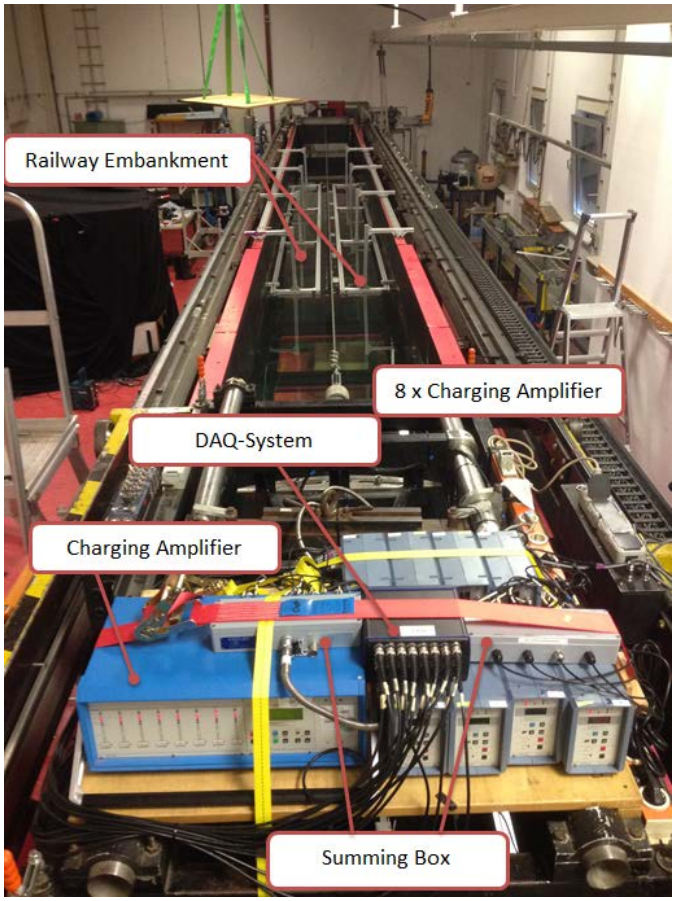

Figure 8: Equipment of the two piezo balances on the test rig

Model Rig/ Piezoelectric balances

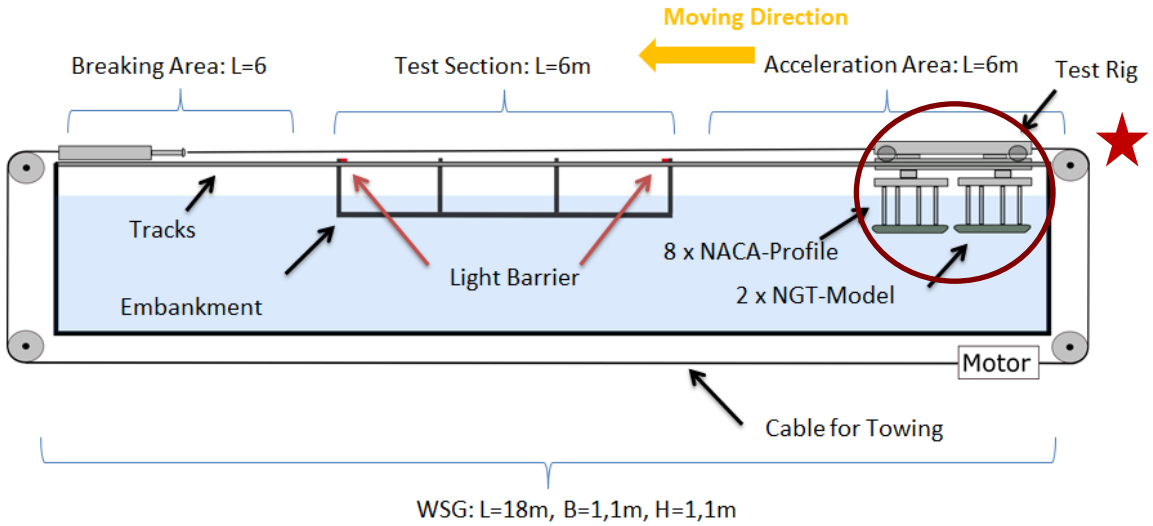

Figure 9: Schematic illustrations of the WSG with test rig and NGT-models

- NGT-Models were installed upside down in the WSG.
- Two piezoeletric balances were used – one for each train.
- Every balance consists of four piezoelectric elements.

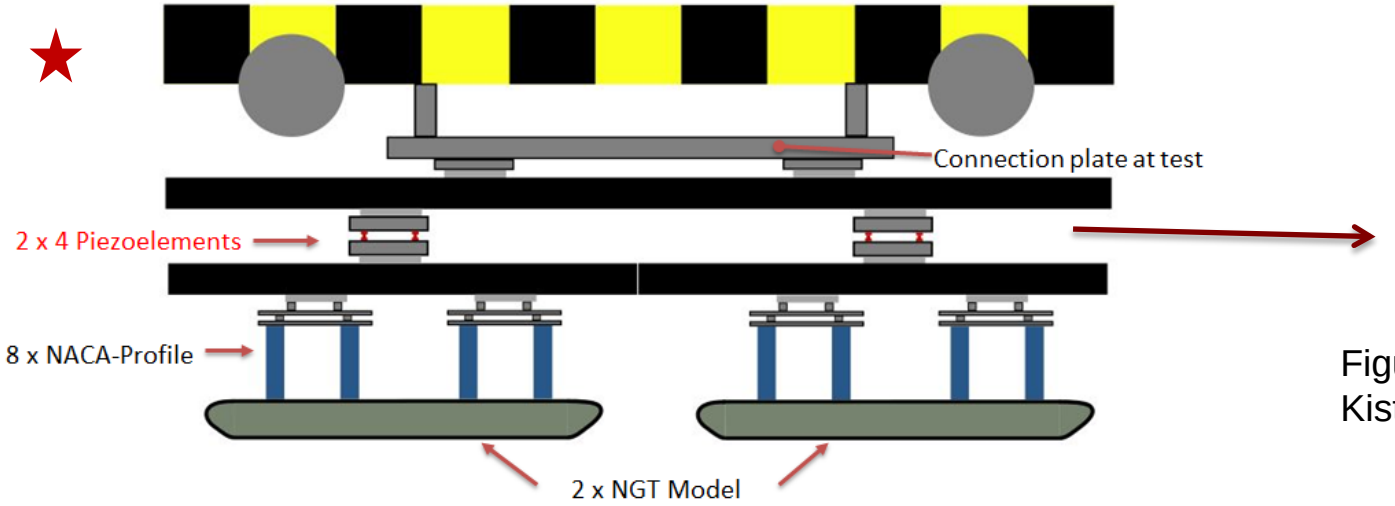

Figure 10: Schematic illustrations of the test rig incl. two Piezoelectric balances

Figure 11: Piezoelectric element, Source: Kistler Instruments

PIV Set-Up

Investigation of the flow field between the trains with PIV

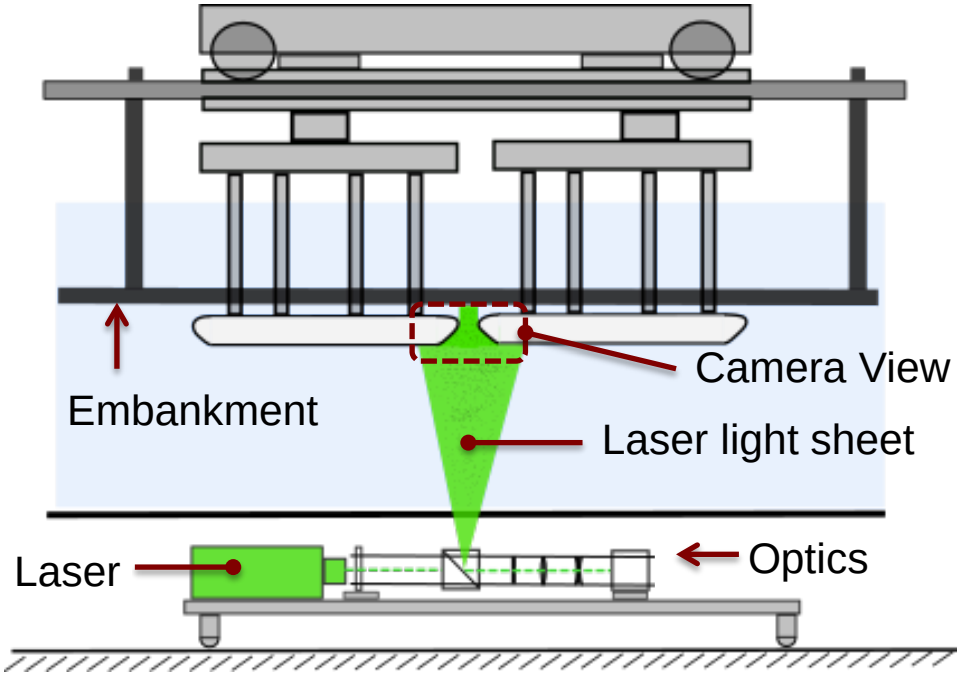

Figure 12: Schematic illustrations of the PIV set-up with the view from the camera position

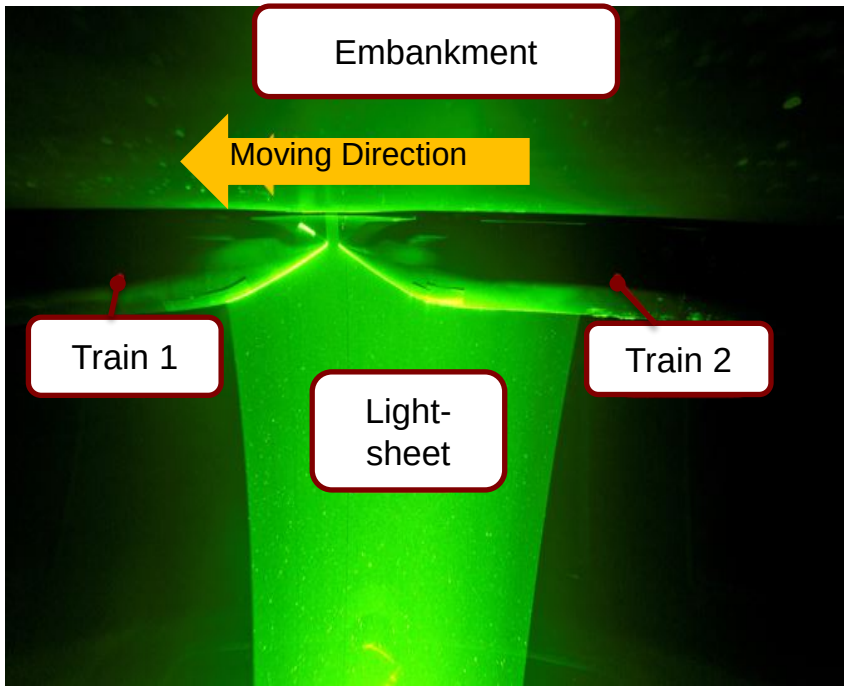

Figure 13: Green PIV-light sheet on NGT models during a PIV measurements

Experimental Parameter

General experimental parameters:

- Two NGT models
- Scale 1:50
- Investigations at six configuration with different distances between the trains (normalised to one train length): x/L=1,2%, x/L=12%, x/L=24%, x/L=36% x/L=48%, x/L=60%
- Flow velocity: 4 m/s
- $Re = \frac{L_C * U_\infty}{\upsilon} = \frac{0{,}06\ m * 4\ m/s}{1{,}004 * 10^{-6}} = 2{,}4 * 10^5$, L_C =characteristic length (train width), U_∞=free stream velocity, υ =kinematic viscosity

Experimental Parameter

Settings for Force Measurements

- Two six-component piezo balances, one for each train
- Sampling frequency: 1 kHz
- 35 runs per configuration

PIV Settings

- Double-pulsed Nd-YAG Innolas Spitlight Laser
- Sampling frequency: 14 Hz
- Tau: 750µs
- PCO Edge Camera
- Field of view: 299 mm x 225mm
- 5,37 pixel/mm
- 20 runs per configuration
- Seeding: Glas balls (diameter: 80-150µm)

Presentation and Discussion of Results

Investigation of the Aerodynamic Drag Coefficient C_D

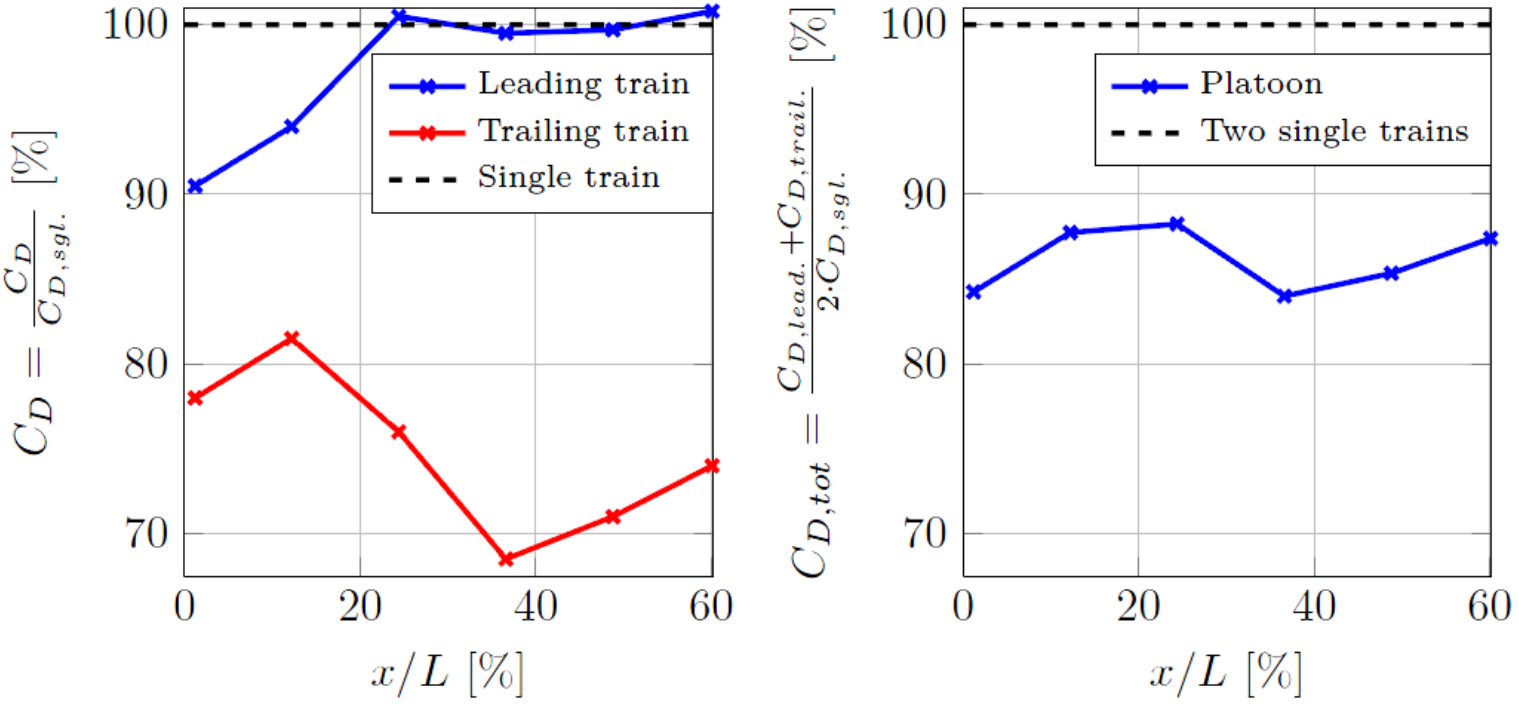

Figure 14: Aerodynamic drag of each train in the platoon (left) and the overall drag of the platoon (right)

- $x/L = 1{,}2\%$: Reduced C_D on both trains, $C_{D,tot}$ reduced by 16 %
- $x/L = 36\%$: Reduced C_D only on trailing train, $C_{D,tot}$ reduced by 16 %
- **Smallest C_D on trailing train occurs at $x/L = 36$ % und $x/L = 48\%$**
- Average reduction of $C_{D,tot}$ of 13,9 %
- Average reduction of C_D on trailing train of 24,4 %

Investigation of the Aerodynamic Drag Coefficient C_D

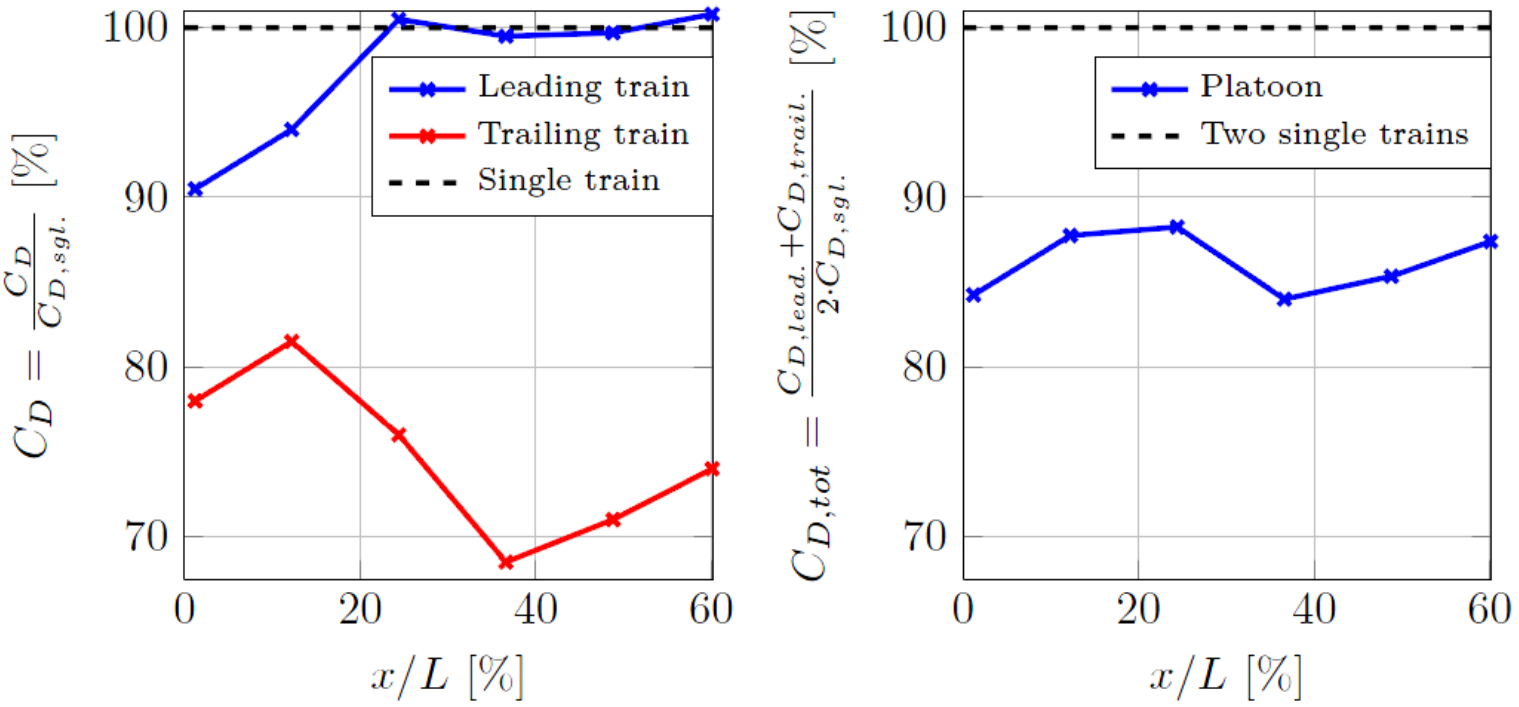

Figure 15: Aerodynamic drag of each train in the platoon (left) and the overall drag of the platoon (right)

Two regions with different effects can be identified:

1. Distances up to x/L=12% where both trains experience reduced C_D → strong interaction

2. Distances greater than x/L=12% where only the trailing train has a reduced C_D → weak interaction

Transient Force Measurement

- Vibrations of the test rig generate interfering frequencies.
- Separating vortices generate force fluctuations with certain a frequency.

→ Mechanical and aerodynamical frequencies have to be identified and distinguished.

- Mechanical induced frequency f_{mech} by the model rig:

$$f_{mech} = \frac{U_\infty}{\pi * d} = \frac{4m/s}{\pi * 0{,}16m} = \frac{1}{0{,}126}s = 7{,}9\ Hz,$$ d= diameter of model rig wheel

- Aerodynamic induced frequencies f_{aero} by seperating vortices:

$$f_{aero} = \frac{Sr * U_\infty}{L_c} = \frac{0{,}1776 * 4\ m/s}{0{,}06m} = 11{,}84\ Hz,$$ Sr= Strouhal number

Frequency Analyses of Transient Force Measurement of F_x at Leading Train

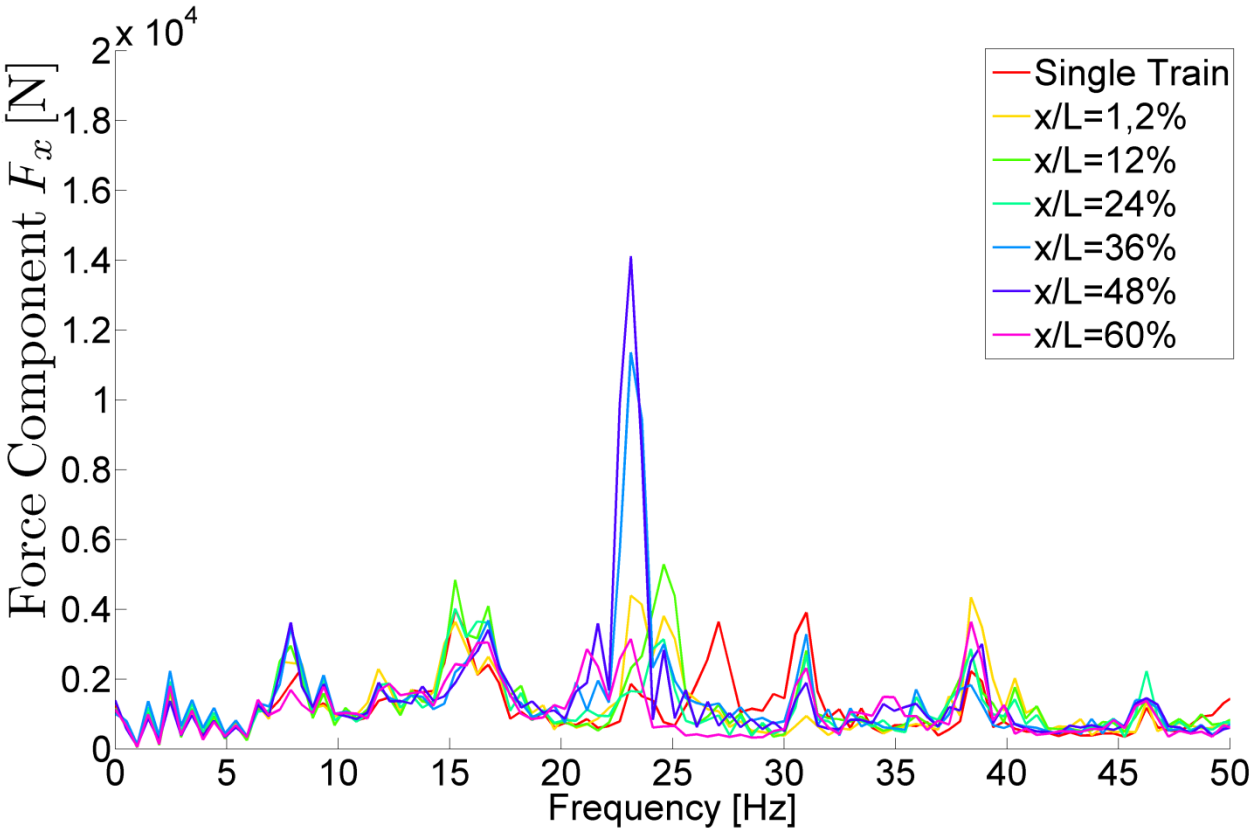

- $f_{mech} = \frac{U_\infty}{\pi * d} = 7{,}9$ Hz
- $f_{aero} = \frac{Sr * U_\infty}{L_c} = 11{,}84$ Hz

Figure 16: Frequency spectrum of transient aerodynamic forces on the leading train

- Small peak at f=7,87 Hz ⟶ f_{mech}
- Further peaks at multiples of f_{mech} ⟶ harmonics of f_{mech} exist (small peaks)

Frequency Analyses of Transient Force Measurement of F_x at Leading Train

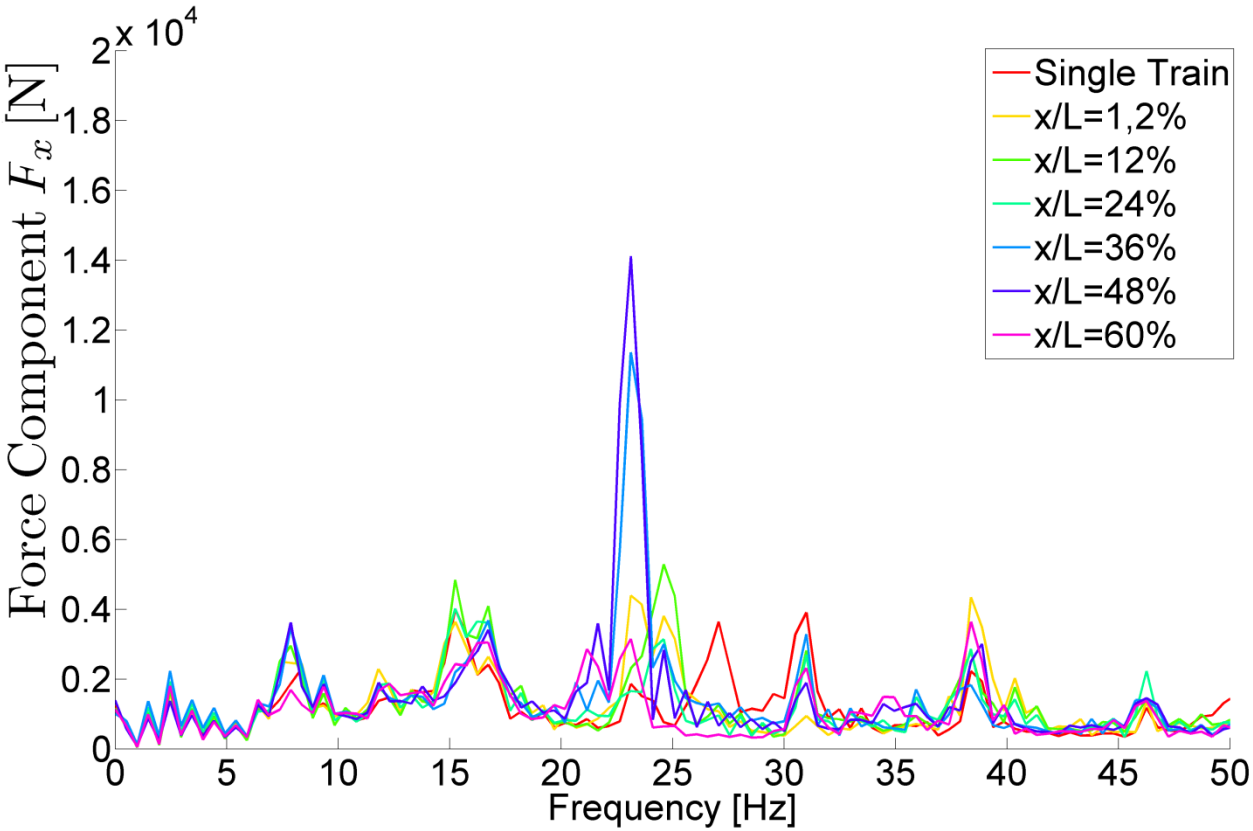

- $f_{mech} = \frac{U_\infty}{\pi * d} = 7{,}9$ Hz
- $f_{aero} = \frac{Sr * U_\infty}{L_c} = 11{,}84$ Hz
- $f = 7{,}87$ Hz ⟶ f_{mech}
- Harmonics of f_{mech} exist

Figure 17: Frequency spectrum of transient aerodynamic forces on the leading train

- No Peak at $f = 11{,}84$ Hz (f_{aero})
- **Peak of F_X at f=23,13 Hz (for x/L=36% und x/L=48%) ⟶ 2 x f_{aero} (large peak)**

Frequency Analyses of Transient Force Measurement of F_y at Leading Train

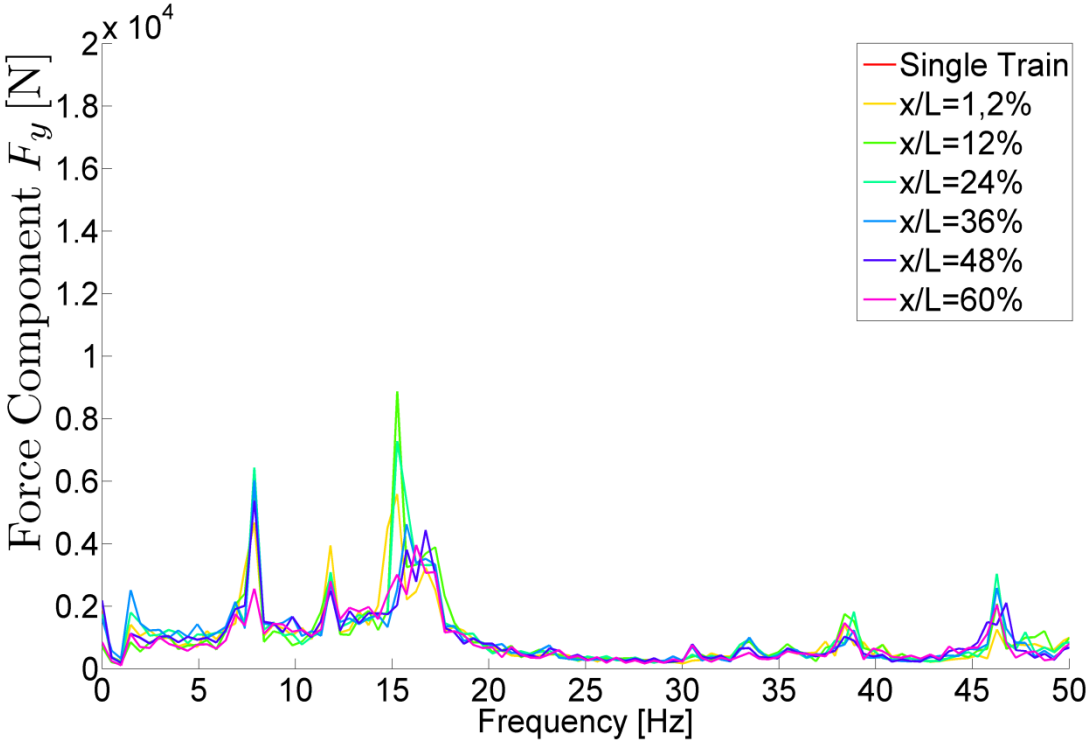

Figure 18: Frequency spectrum of transient aerodynamic forces F_y on the leading train

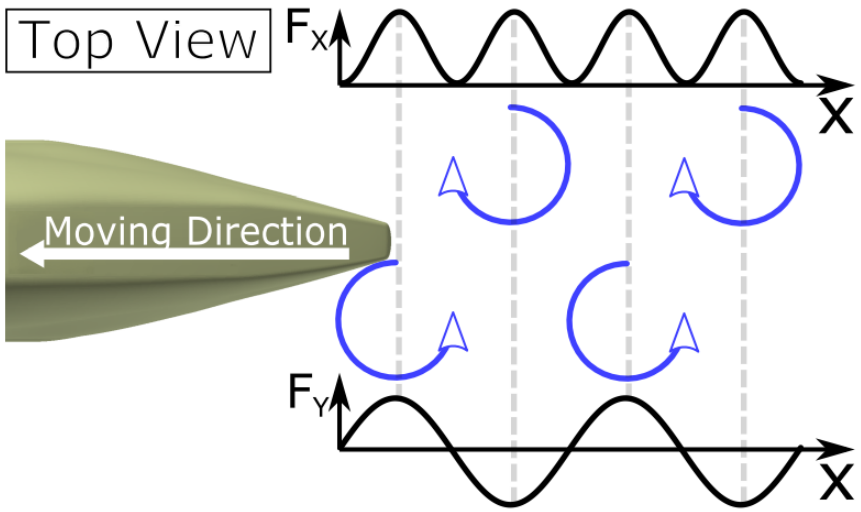

Figure 19: Theoretical Scheme of separating vortices in the wake and the resulting force components

- No Peak at f=23,13 Hz, but at f= $\frac{23{,}13\ \text{Hz}}{2}$ = 11,55 Hz
- F_X appear in FFT with twice the frequency of F_Y

  → The period length of F_Y is double of F_X (see fig. 19)

Velocity Fields (PIV)

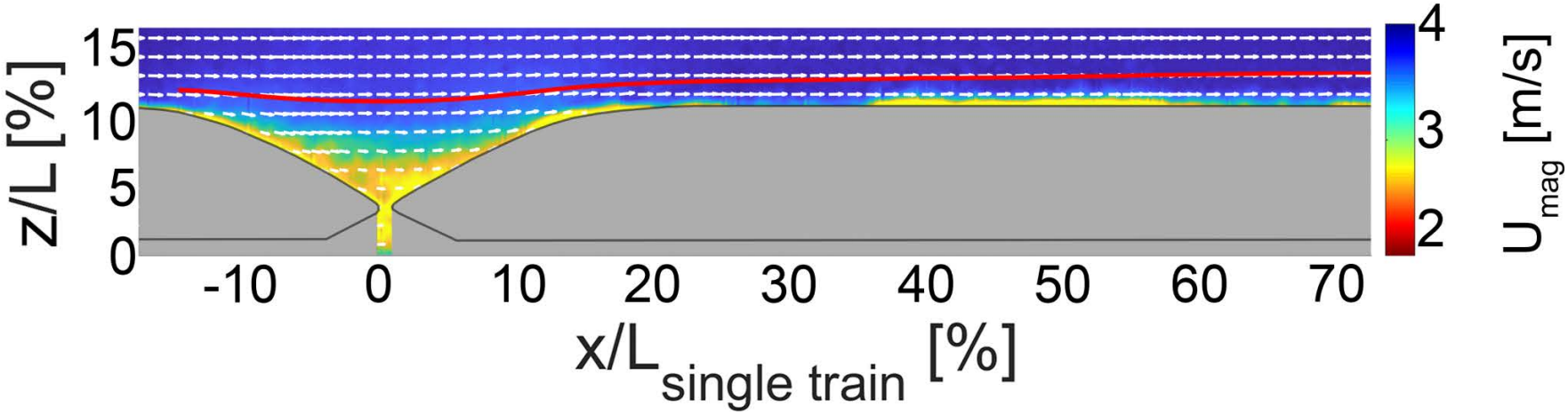

Figure 20: Velocity field and velocity magnitude of two trains with a distance of x/L=1,2% of one train length

- Mostly low velocity between the trains, streamline remains on nearly on same vertical level
- Connected field of low velocity can indicate strong interactions
- Low velocity leads to small stagnation pressure → drag reduction at trailing train
- Gap too small to form a typical wake → models act aerodynamically like one train

Velocity Fields (PIV

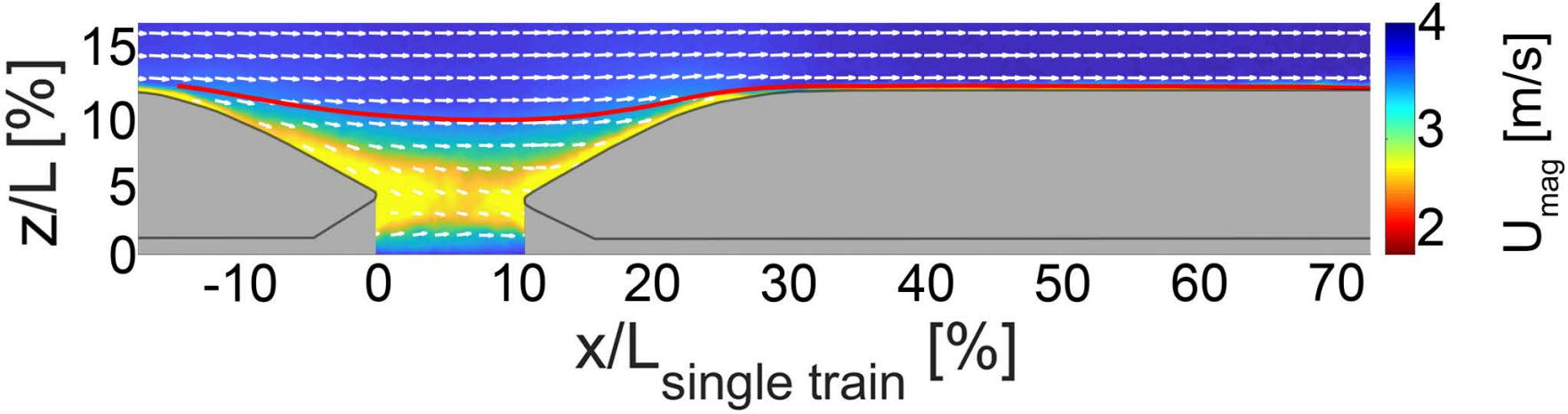

Figure 21: Velocity field and velocity magnitude of two trains with a distance of x/L=12% of one train length

- Streamline narrows down into the wake ⟶ lower pressure between the train
- Strongly connected fields with low relative velocity between the trains

  ⟶ appearance of strong interaction
- Low velocity leads to low stagnation pressure at tip of trailing train ⟶ drag reduction

Velocity Fields (PIV)

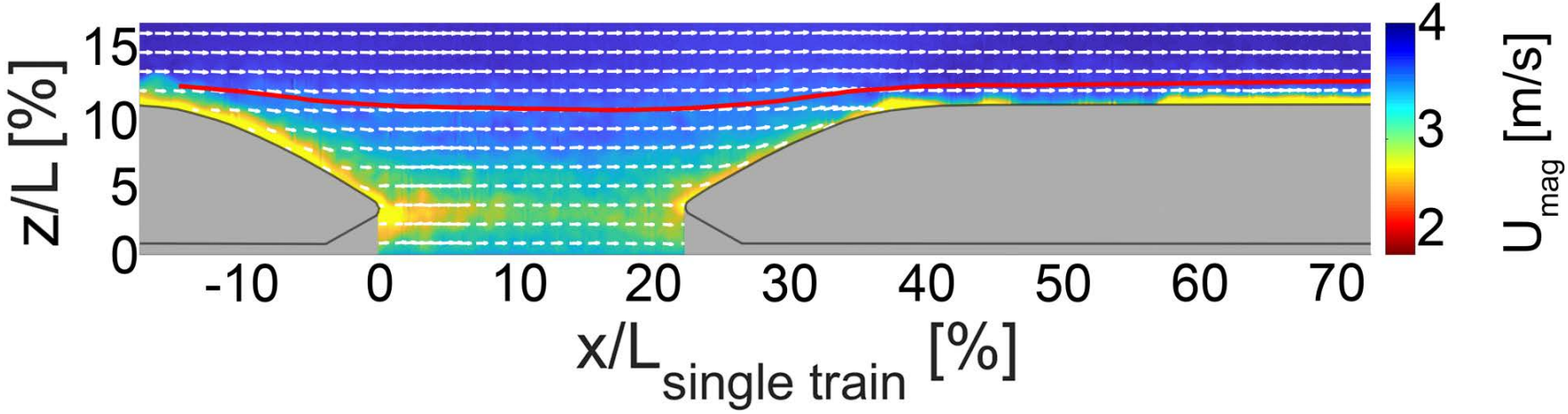

Figure 22: Velocity field and velocity magnitude of two trains with a distance of x/L=24% of one train length

- Lower magnitude at near-wall region in wake → similar to a single train
- Higher velocity in the wake far field
- Increasing relative velocity between the trains compared to configurations with smaller gaps
  → higher stagnation pressure on trailing train
- “weak interaction”

Vorticity Fields (PIV)

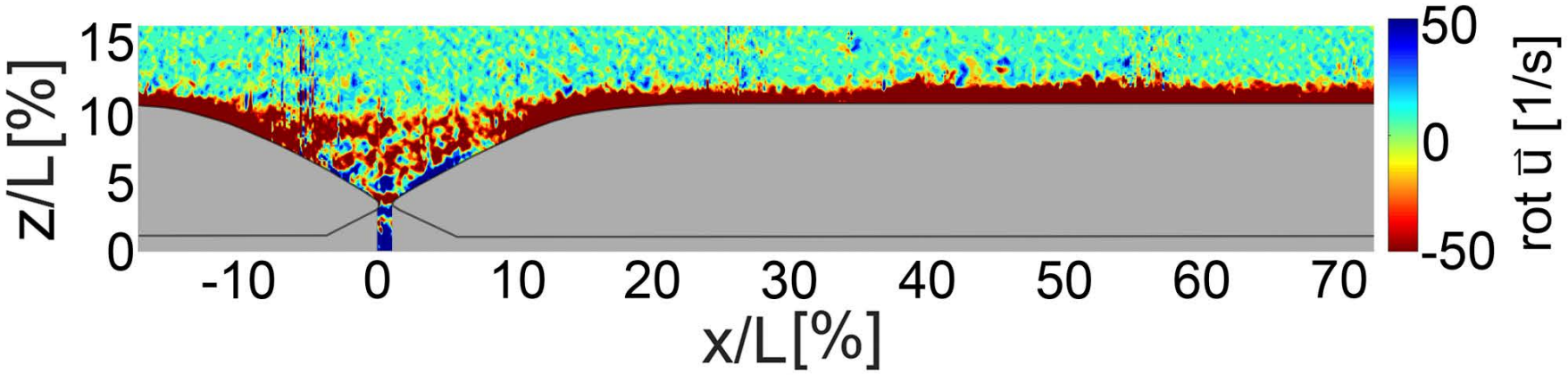

Figure 23: Vorticity of the velocity field of two trains with a distance of x/L=1,2% of one train length

- Almost exclusively negative rotational movement
- Vorticity in top section of the trains are most likely created by a shear layer and turbulences in the close-by region
- Not enough distance between the trains to form a typical wake

  → Configuration shows aerodynamic behaviour of two mechanically coupled trains

Vorticity Fields (PIV)

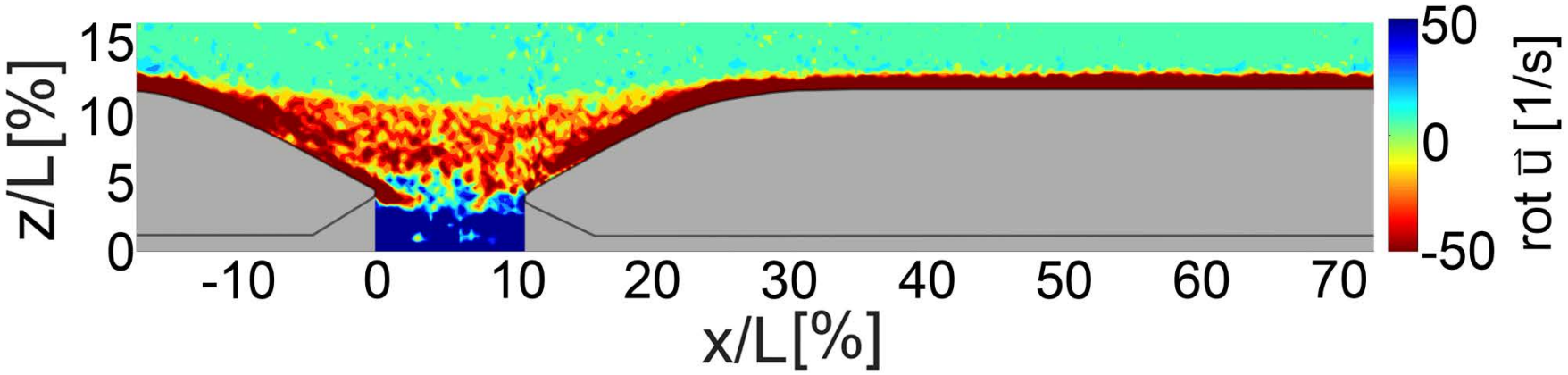

Figure 24: Vorticity of the velocity field of two trains with a distance of x/L=12% of one train length

- Strongly connected vorticity with regions of negative value in top section
  → Appearance of Strong Interactions
- Vorticity is most likely created by a shear and also separating vortices at the rear of the train.
- Positive rotational movement of vorticity in bottom section which is most likely caused by the underfloor flow.
- Higher intensity of turbulence → slightly higher drag

Vorticity Fields (PIV)

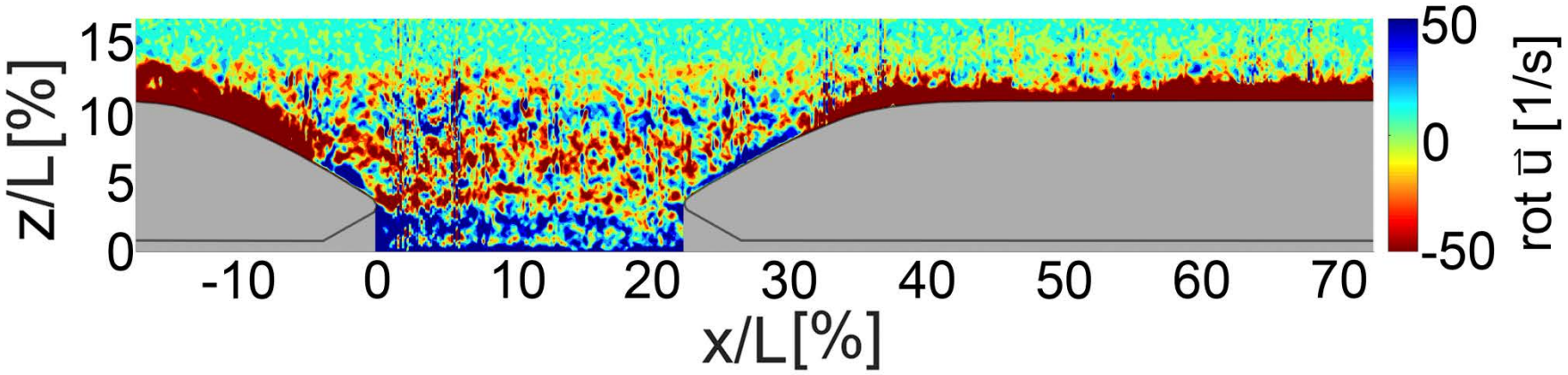

Figure 25: Vorticity of the velocity field of two trains with a distance of x/L=24% of one train length

- No connected field of vorticity with same directional movement (mixed fields)
- Higher values of rot $\vec{u}$ in near-wall region
- Start of dissipation of vortices
- Vanishing of strong aerodynamic interactions between the trains (weak interactions)

  → drag of trailing increases, drag of leading train decreases

SUMMARY

1. Can the aerodynamic drag be reduced by Virtual Coupling and what unsteady aerodynamic forces do occur?

   - ✓ The aerodynamic drag is reduced by Virtual Coupling.
   - ✓ Overall Drag experiences a reduction of 13,9% (12%-16% depending on configuration).
   - ✓ Average drag reduction of the trailing train of 24,4% (18%-30.5% depending on configuration).
   - ✓ Drag decreases on both trains at configurations with distances up to x/L=12% of one train length → strong interaction

2. Are the any correlations between the unsteady aerodynamic forces and the aerodynamic drag?

   ✓ Configurations with dominant signals in the FFT's also show the lowest drag of the trailing train (x/L=36% und x/L=48%).

3. What effect has the flow between the two trains on the aerodynamic forces?

   ✓ Lower relative velocity in the wake → lower stagnation pressure, thus lower drag

   ✓ Intensity of turbulence → higher turbulences seem to slightly increase the drag

4. How does the distance between the trains affect the aerodynamic forces?

- ✓ Strong Interactions (at distances up to x/L=12%)
  - ⟶ reduced drag on both trains
- ✓ Weak Interactions (at distances larger than x/L=12%)
  - ⟶ reduced drag only on trailing train
- ✓ Distance between the train effects the relative velocity in the wake of the first train as well as the intensity of turbulences acting on the trailing train.

QUESTIONS

Thank you for you attention!

Feel free to ask question!

REFERENCES / Literature

[1] G. F. Romberg, F. Chianese, and R. G. Lajoie. 2015. “Aerodynamics of race cars in drafting and passing situations”. SAE Technical Paper. No. 710213.

[2] K. Koenig and A. Roshko. 1985. “An experimental study of geometrical effects on the drag and flow field of two bluff bodies separated by a gap”. *Journal of fluid mechanics*. no. 156. 167–204.

[3] M. Zabat, N. Stabile, S. Farascaroli, and F. Browand. 1995. The aerodynamic performance of platoons: A final report. Research Report. California Partners for Advanced Transit and Highways (PATH). University of California, Berkeley

[4] P. Jootel. 2014. Safe road trains for the environment - project final report. Research Report. Satre Project. [Online]. Available: http://sartre -project.eu/en/publications/Documents/SARTRE_Final-Report.pdf.

[5] T. Thieme. Aerodynamische Untersuchung von Hochgeschwindigkeitszügen beim dynamischen Flügeln mittels Piezowaagen und PIV. 2016. Master Thesis. Technische Universität Ilmenau.

[6] Thomas W. Muld, Gunilla Erfraimsson and Dan S. Henningson. „Wake characteristics of high-speed trains with different length“. 2013. Proceedings of the Institutions of Mechanical Engineers. Part F: Journal of Rail and Rapid Transit. No. 228(4). 333-342

REFERENCES / Pictures

[6] https://totalwomenscycling.de/rennrad/rr-fahrtechnik/windschatten-fahren-ratgeber-32745/ (Accessed: 15.01.2018)

[7] https://www.nascar.com/en_us/news-media/articles/2011/04/20/inside-nascar-science-draft.html) (Accessed: 15.01.2018)

[8] http://www.bahnbilder.de/bild/deutschland~dieseltriebwagen--95-80-~br-0-605-ice-td/149212/605-507-am-07112007-in-padborg.html (Accessed: 15.01.2018)

[9] Ben Schaub, DLR Train Couple Test. 2016. Daily Planet – Discovery Channel.

Frequency Analyses of Transient Force Measurement of F_x at Trailing Train

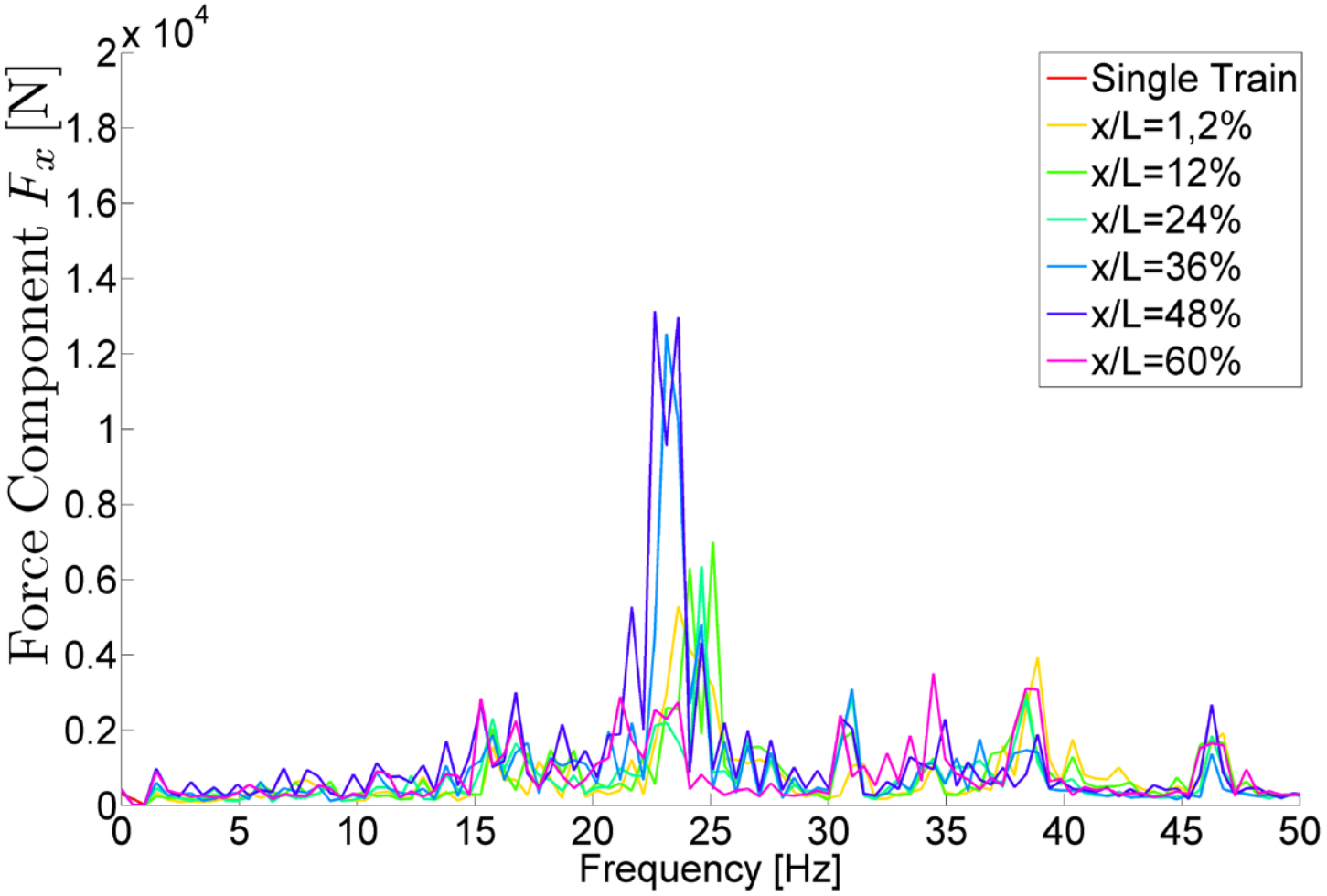

Figure 26: Frequency spectrum of transient aerodynamic forces F_y on the trailing train

Frequency Analyses of Transient Force Measurement of F_y at Trailing Train

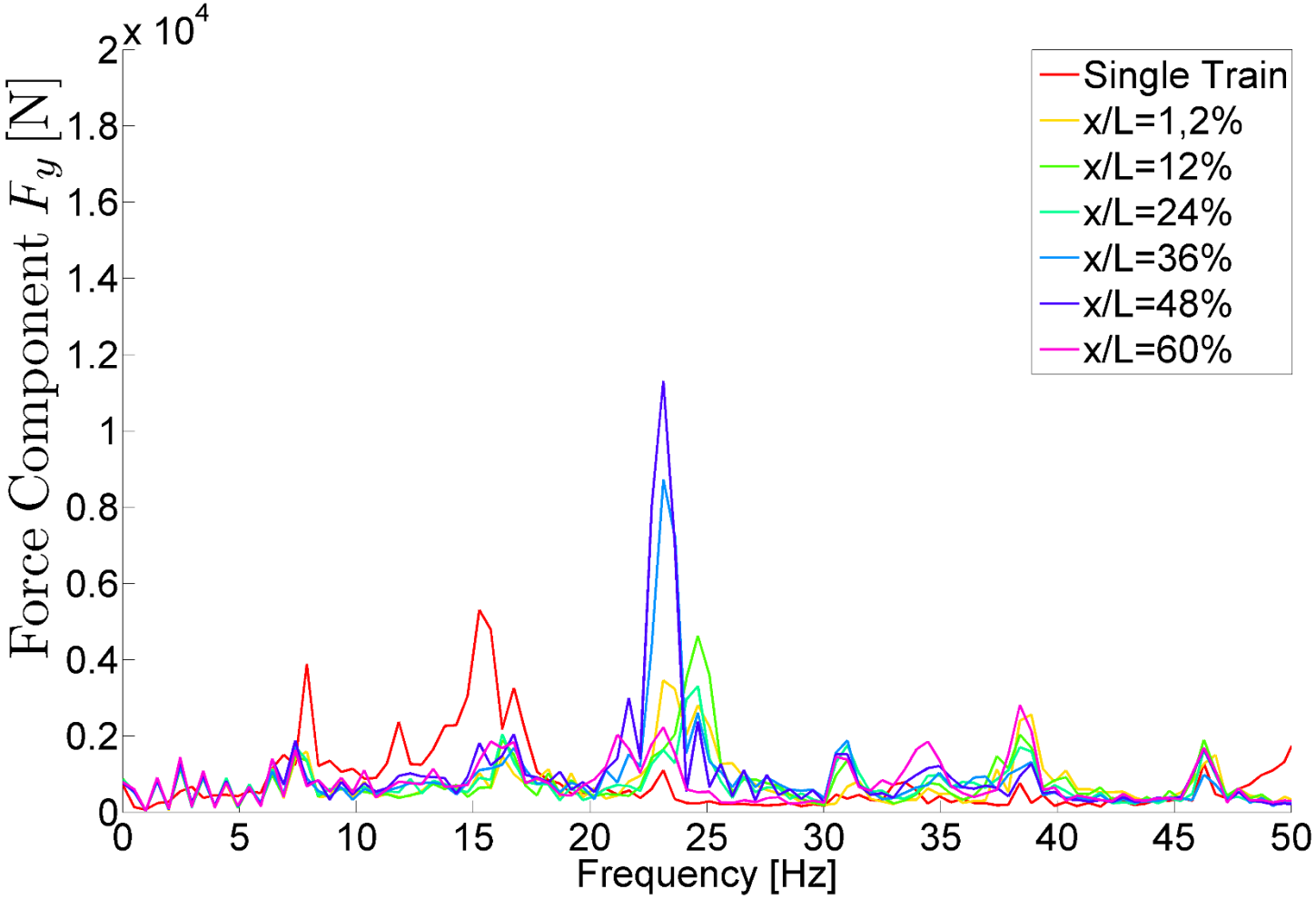

Figure 27: Frequency spectrum of transient aerodynamic forces F_y on the trailing train

Velocity Fields (PIV)

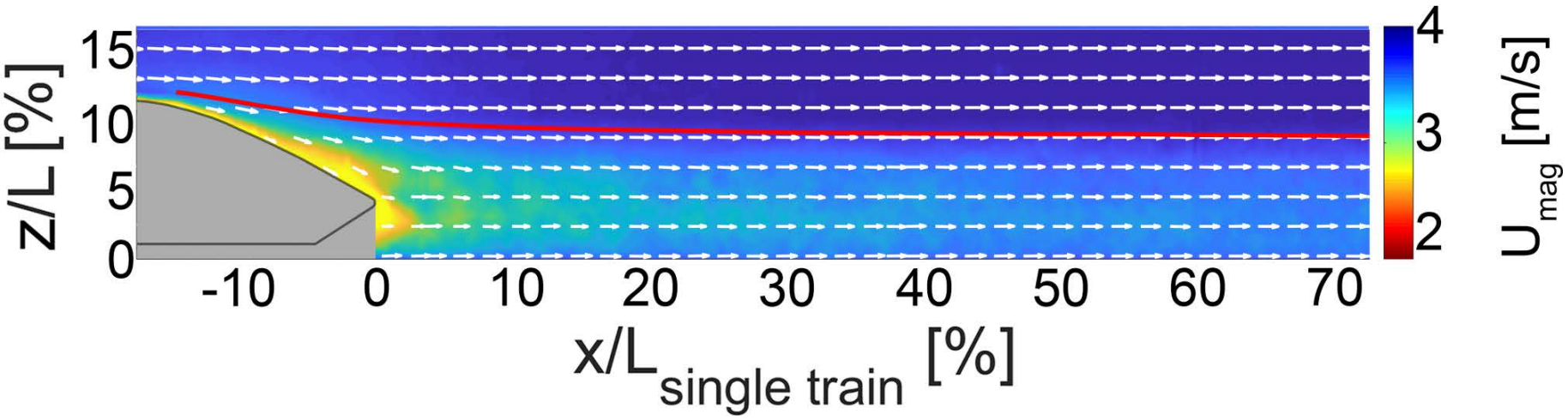

Figure 29: Velocity field and velocity magnitude for a single train measured in a vertical light sheet (Reference case)

Velocity Fields (PIV)

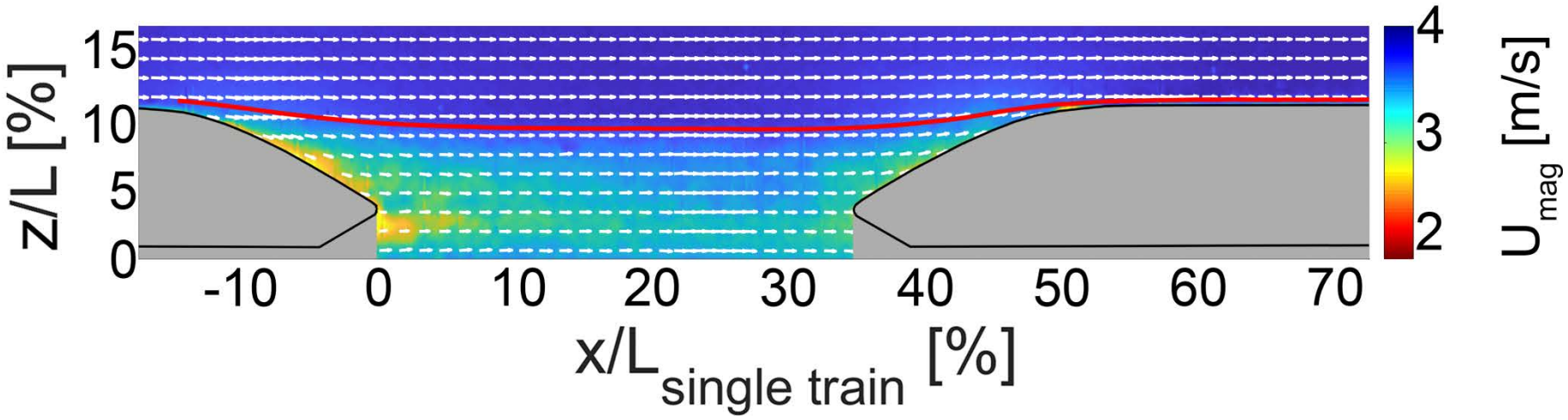

Figure 29: Velocity field and velocity magnitude of two trains with a distance of x/L=36% of one train length

Velocity Fields (PIV)

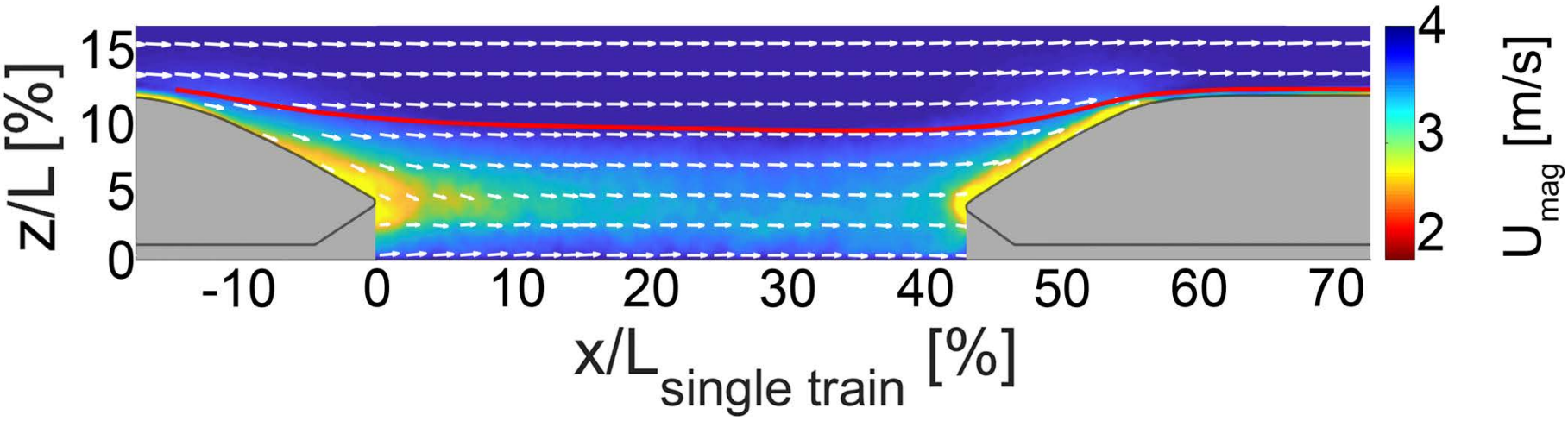

Figure 30: Velocity field and velocity magnitude of two trains with a distance of x/L=48% of one train length

Velocity Fields (PIV)

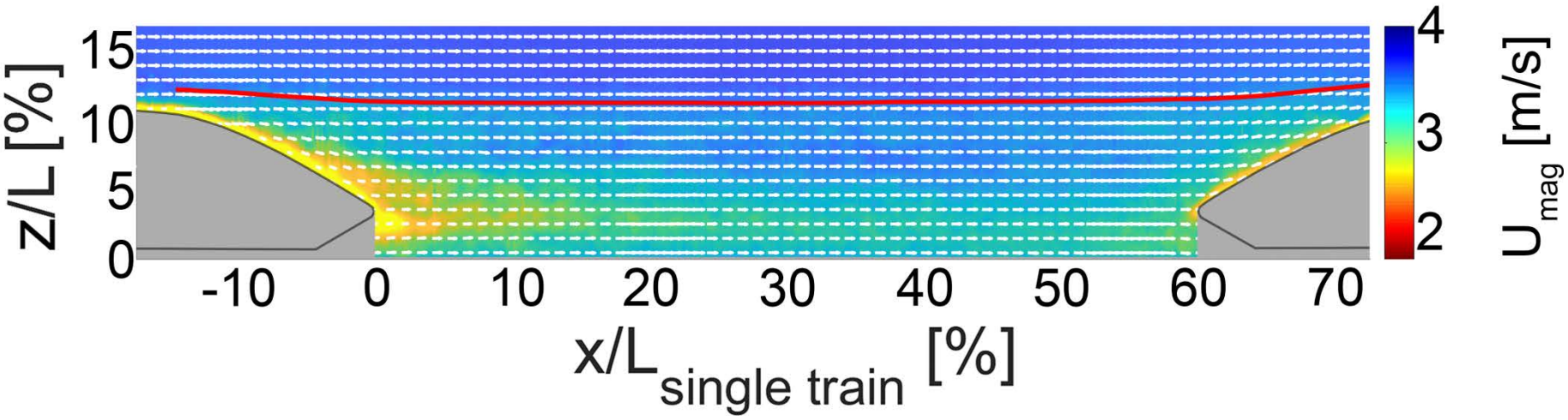

Figure 31: Velocity field and velocity magnitude of two trains with a distance of x/L=48% of one train length

Vorticity Fields (PIV)

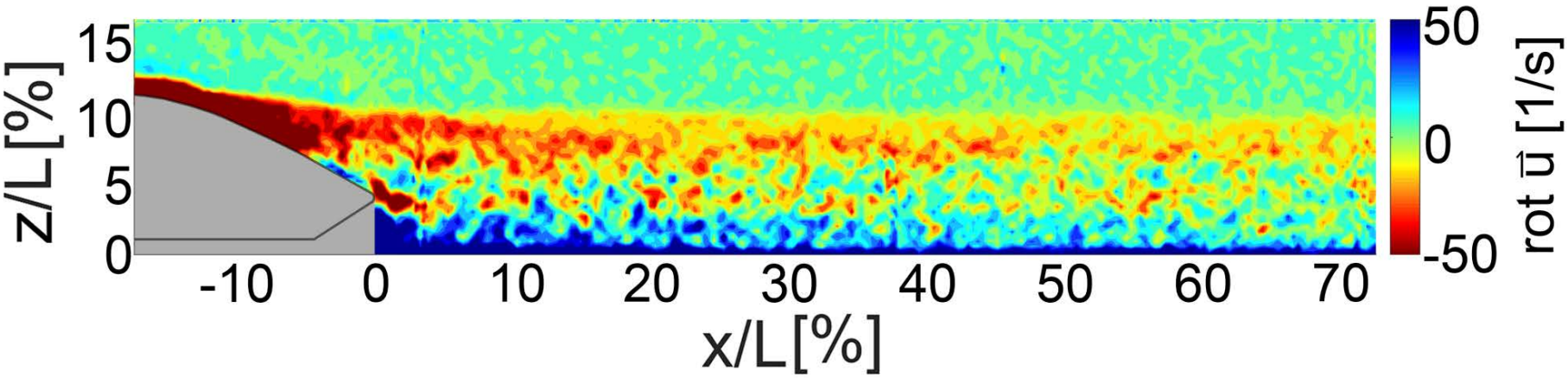

Figure 32: Vorticity of the velocity field of a single train

Vorticity Fields (PIV)

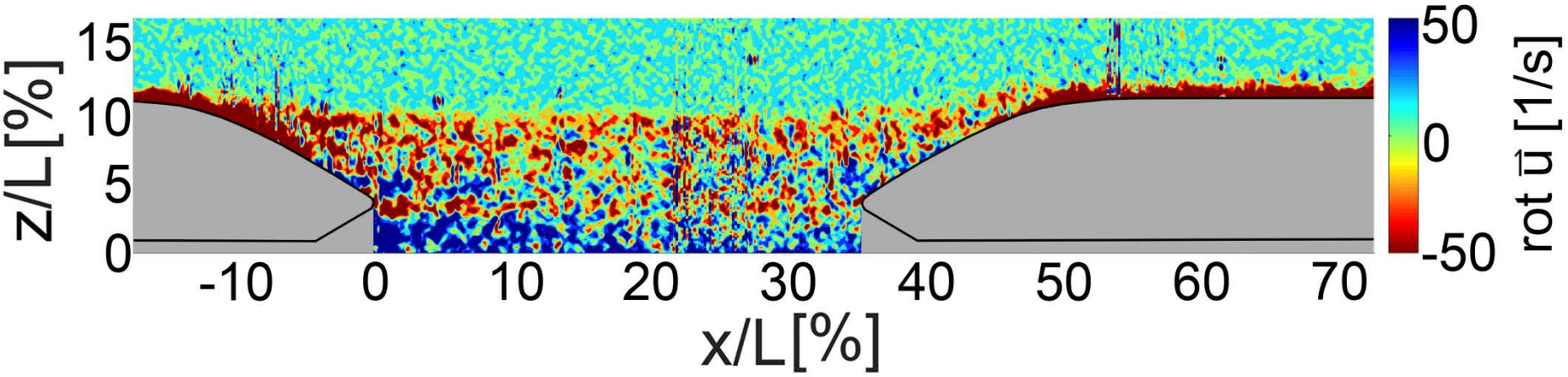

Figure 33: Vorticity of two trains with a distance of x/L=36% of one train length

Vorticity Fields (PIV)

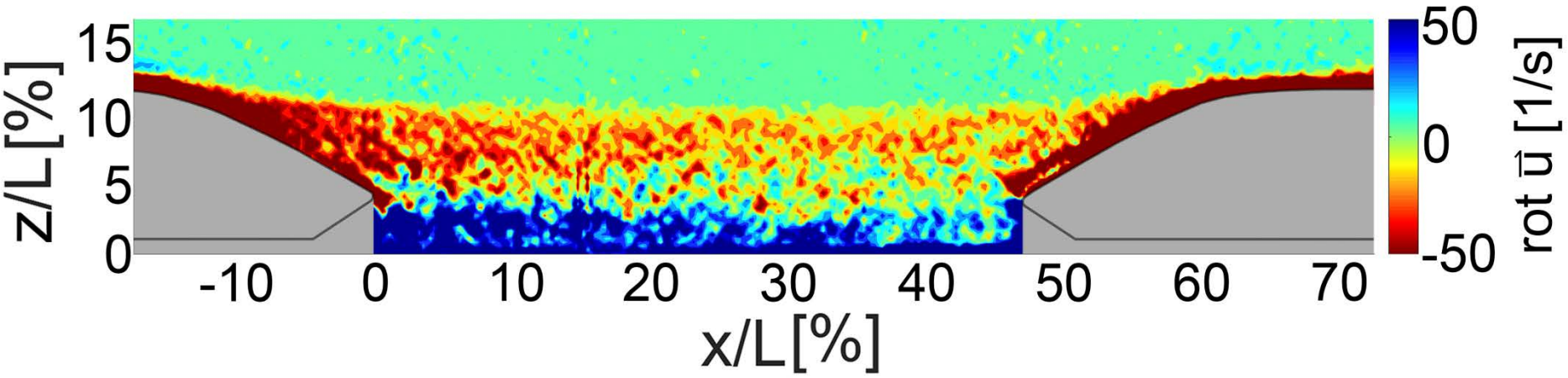

Figure 34: Vorticity of two trains with a distance of x/L=48% of one train length

Vorticity Fields (PIV)

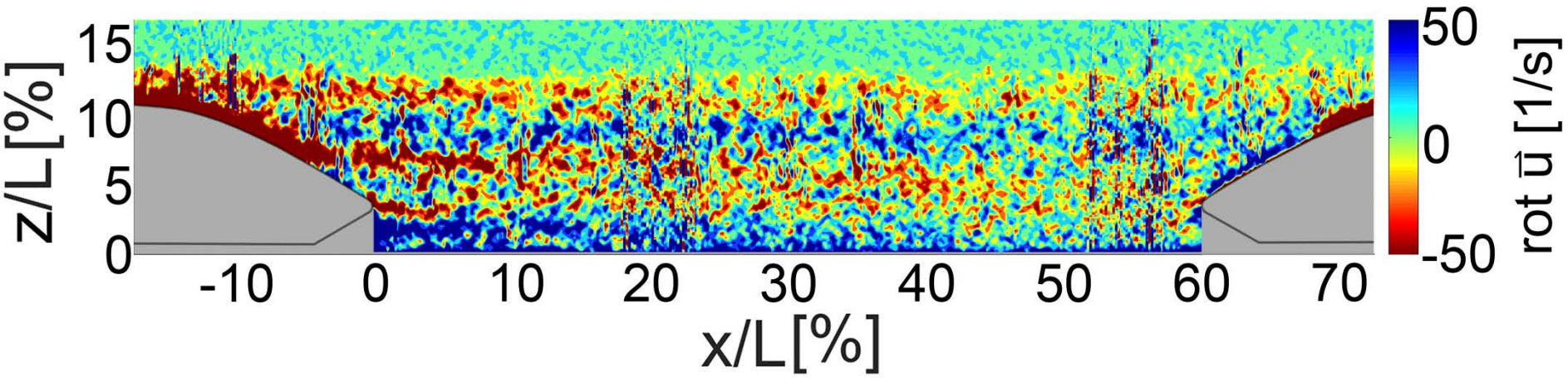

Figure 33: Vorticity of two trains of a single train

Determination of the Strouhal Number by Extrapolation

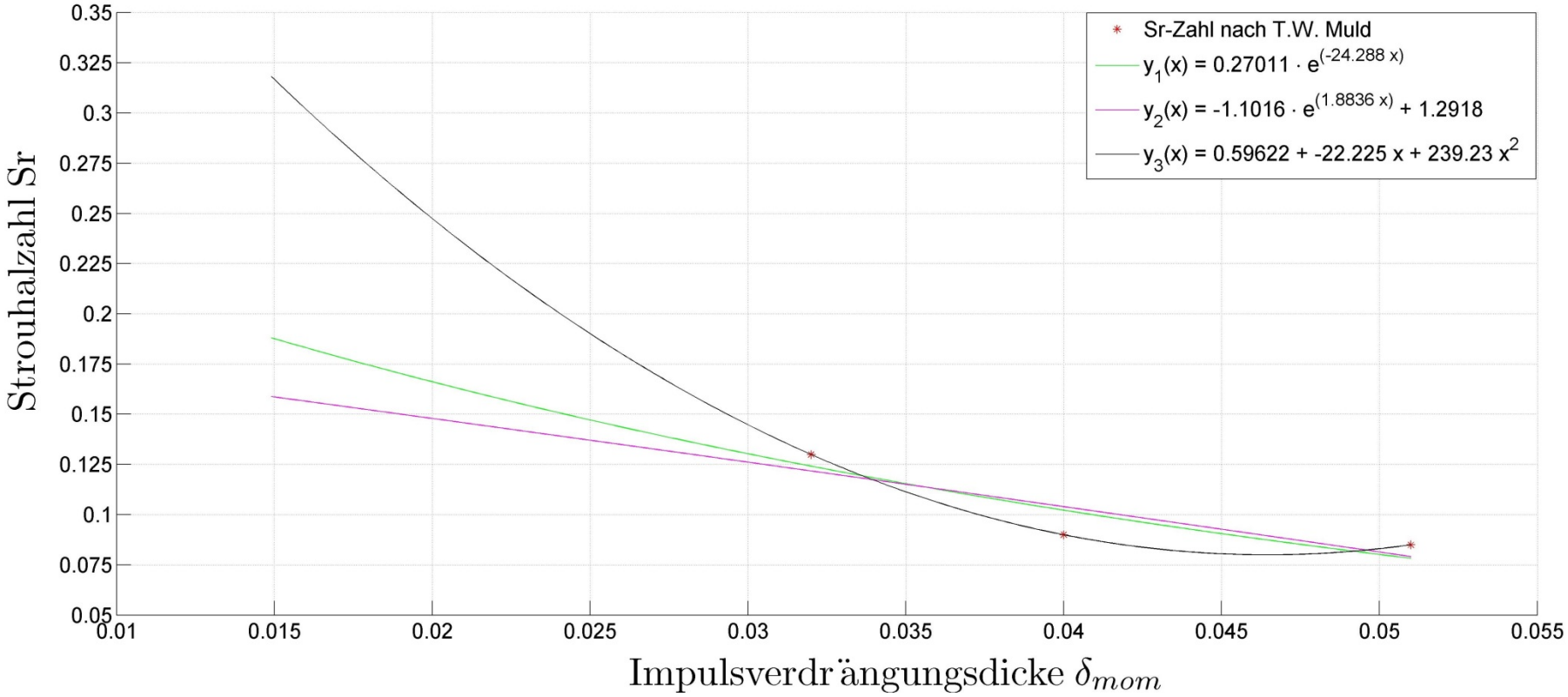

Figure 36: Extrapolated values for the Strouhal Number based on data von T. W. Muld (T.W.Muld et. al., 2013) and the geometry of the NGT train model by means of three different fit functions